

Massive Compact Halo Objects

Chengchao Yuan and Scott Langdon

Abstract

In this report we discuss some aspects of Massive Compact Halo Objects (MACHO) such as how to detect them, assumptions which place constraints on the fraction of dark matter in MACHOs, and some aspects of the mechanics of systems which include MACHOs.

1 Microlensing Constraints

The physical nature of dark matter has been an old enigma since the early studies toward galaxy cluster masses and galaxy rotation curves. Possible candidates of dark matter could be weakly interacting massive particles (WIMPs), such as axions and neutrinos, and MACHOs. One attractive and wide-used method for searching MACHOs was firstly proposed by Paczynski in 1986, which is now called microlensing method.

Consider the situation that a light beam from a star at distance L is deflected by a lensing object of mass m and distance x . As a result, the brightness of the star is amplified by a factor A

$$A = \frac{u^2 + 2}{u(u^2 + 4)^{1/2}} \quad (1)$$

where $u = b/R_E$, b is the impact parameter and R_E is the Einstein radius, which encodes the physical information of lensing objects

$$R_E = 2\sqrt{\frac{Gmx(L-x)}{c^2L}}. \quad (2)$$

Hence, for a given source with known position (can be used to determine b) and distance (L), the measurements on its light curve enable us to infer A and further the mass of MACHO, m .

In practice, the amplification on the magnitude we measured is a consequence of the lensing effect contributed from all MACHOs on the line-of-sight. It is more important to estimate the number of MACHOs that could influence one specific microlensing event for one given threshold A_{TH} , or equivalently $b_{TH} = u_{TH}R_E$ which defines a tube. Here, the number of MACHOs inside the tube is called optical depth τ and obviously it is an integral of number density over the whole tube on the line-of-sight, e.g.

$$\tau = \int_0^L \frac{\rho(\mathbf{r})}{m} \pi u_{TH}^2 R_E^2(\mathbf{r}) dr. \quad (3)$$

To constrain the halo mass, we need to assume a density profile $\rho(\mathbf{r})$. Kim Griest studied two different density profiles

$$\rho(r) = \rho_0 \frac{a^2 + r_0^2}{a^2 + r^2}$$

when $a = 0$ and $a \sim 2 - 8$ kpc. From his result, the dependence on the values of a is not sensitive. However we should keep this uncertainty in mind if we apply τ to constrain the MACHO mass and fraction.

In 2000, C. Alcock et al.[2] presented their experiment on microlensing toward the Large Magellanic Cloud (LMC). They analyzed the 5.7 years of photometry on 11.9 million stars in LMC and finalized 13-17 microlensing events. Figure 1 shows the light curves for one event, for illustration purpose. The fit of to a microlensing takes the form

$$f_R(t) = A(t)f_{0R}, \quad f_B(t) = A(t)f_{0B}, \quad A(t) = A(u(t))$$

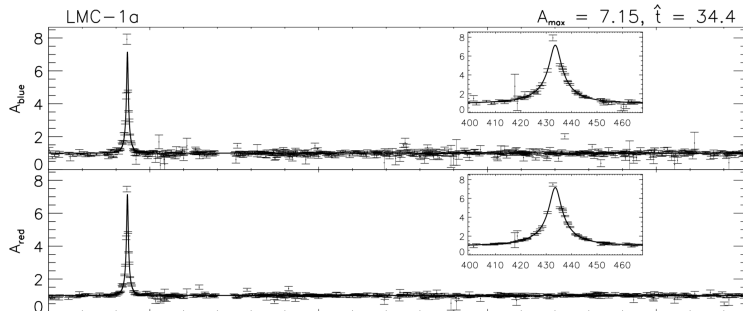


Figure 1: Light curves for one microlensing event. Upper and lower panels correspond to the observations in blue and red passbands.

$$u(t) = \sqrt{u_{min}^2 + 4\left(\frac{t - t_{max}}{t}\right)^2}$$

where f_{0R} , f_{0B} are baseline fluxes in red and blue passbands, u_{min} corresponds to the minimal impact factor after the MACHO enters the lensing tube. In the figure, the maximum amplification factor A_{max} is achieved when $u = u_{min}$. Typically, $u_{min} \neq 0$ considering the density of MACHOs in the tube may not such high that the lensing object is on the ligh between the observer and the background star. The Einstein radius crossing time $\hat{t} = 2r_E/v_{\perp}$.

The microlensing rate $d\Gamma/dt$ is model dependent comparing to τ and is often used to constrain the MACHO mass and halo fraction f . Once the model is specified, Γ depends on the event time scale and their velocity distribution of MACHOs. The average number of observed events is then

$$N_{exp} = E \int_0^{\infty} \frac{d\Gamma}{dt} \epsilon(t) dt$$

where $E = 6.12 \times 10^7$ object-years is the exposure time and $\epsilon(t)$ is the detection efficiency. Since the time scale of microlensing $\propto r_E/v$ is proportional to $m^{1/2}$, it is possible to use the observed time scales to constrain MACHO mass. In the paper by C. Alcock et al., a two parameter model (m , f) where where a fraction f of the dark halo is made of MACHOs with a mass m while the remaining $1 - f$ of the halo is assumed to be in MACHOs outside the mass range. The likelihood of observing a sample of N_{obs} events with time scale \hat{t}_i , $i = 1, 2, \dots, N_{obs}$ is given by

$$L(m, f) = \exp(-N_{exp}) \prod_{i=1}^{N_{obs}} \left[E \epsilon(\hat{t}_i) \frac{d\Gamma}{dt}(\hat{t}_i, m) \right]. \quad (4)$$

Explicit expressions for $d\Gamma/dt$ and $\epsilon(t)$ are given by [4] and [2]. A constraint on the $m - f$ plane can be obtained by maximizing the likelihood. The constraints using 17 events are shown in Fig. 2.

2 Cluster Heating by MACHOs

The dynamic environment of a star cluster leads to an interchange of velocities among the components of the cluster. If some of those objects are MACHOs, their energy can be interact with the stars of the cluster. According to [3], when a range of masses is present interactions lead to mass segregation where the most massive bodies have the most spatially compact distribution, leading to less massive objects, on average, to have a less compact distribution. If the cluster contains stars and more massive MACHOs, this interchange can lead to the distribution of the stars becoming less compact over time.

In [3] a single star cluster near the center of recently-discovered faint dwarf galaxy, Eridanus II, is used to compare measured half-light radius vs that predicted by the presence of MACHOs of significantly more mass than the stars.

The change in half-light radius ϵ of the cluster over time can be predicted by the change in kinetic energy of the visible stars. Again following [3] the change in half-light radius can be calculated as follows.

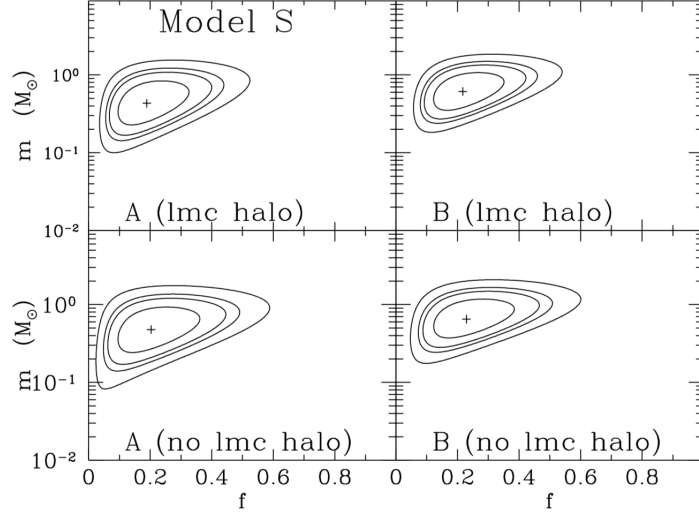


Figure 2: Likelihood contours for MACHO mass m and halo fraction f for model S, which has a typical size halo. The plus sign shows the maximum-likelihood estimate, and the contours enclose regions of 68%, 90%, 95%, and 99% probability. The panels are labeled according to which set of selection criteria (A or B) is used, and whether or not a LMC halo with MACHO fraction f is included.

The diffusion coefficient is given by

$$D[(\Delta v)^2] = \frac{4\sqrt{2}\pi G^2 f_{DM} m_a}{\sigma} \ln \Lambda \left[\frac{\text{erf}(X)}{X} \right], \quad (5)$$

where

$G = 6.67408 \text{ km}^3/\text{kg}/\text{s}^2$ (gravitational constant),

m_a = MACHO mass,

σ = MACHO velocity dispersion,

f_{DM} = fraction of DM mass in MACHOs of mass m_a , taken to be 1 here,

ρ = total dark matter density in the cluster,

$\ln \Lambda$ = Coulomb logarithm,

X = ratio of stellar velocity to MACHO velocity, here assumed to be small,

$\text{erf}(X)/X \approx 1$ because X small.

For the Coulomb logarithm the author uses $\ln \Lambda \approx \ln \left(\frac{r_h \sigma^2}{G(m+m_a)} \right)$, where r_h is the half-light radius of the cluster and m is the mass of the cluster stars.

With these values eq. 5 becomes:

$$D[(\Delta v)^2] = \frac{4\sqrt{2}\pi G^2 f_{DM} m_a}{\sigma} \ln \left(\frac{r_h \sigma^2}{G(m+m_a)} \right). \quad (6)$$

Eq. 6 represents the incremental change in system velocity for MACHO mass of m_a for an incremental unit of time. But in this case, all of the MACHO mass is assumed to be at m_a , $D[(\Delta v)^2]$ expresses the change in kinetic energy. Using eq. 6 and the Virial theorem, which relates the total average kinetic energy of a stable system of particles to the total potential energy, here: $\frac{U}{M} = \text{constant} - \alpha \frac{GM_*}{r_h} + \beta G \rho r_h^2$, the change in half-light radius, which is inversely proportional to kinetic energy in the visible stars,

can be expressed:

$$\begin{aligned}\frac{dr_h}{dt} &= \frac{4\sqrt{2}G^2 f_{DM} m_a}{\sigma G} \ln\left(\frac{r_h \sigma^2}{G(m+m_a)}\right) \left(\alpha \frac{M_*}{\rho r_h^2} + 2\beta r_h\right)^{-1} \\ &= \frac{4\sqrt{2}G f_{DM} m_a}{\sigma} \ln\left(\frac{r_h \sigma^2}{G(m+m_a)}\right) \left(\alpha \frac{M_*}{\rho r_h^2} + 2\beta r_h\right)^{-1}.\end{aligned}$$

Which can be solved numerically. A good way to solve this might be a Runge-Kutta 4th order method, but here, for simplicity, I simply write:

$$\Delta r_h = \frac{4\sqrt{2}G f_{DM} m_a}{\sigma} \ln\left(\frac{r_h \sigma^2}{G(m+m_a)}\right) \left(\alpha \frac{M_*}{\rho r_h^2} + 2\beta r_h\right)^{-1} \Delta t \quad (7)$$

and solve by taking small increments of Δt .

Figure 3 shows the evolution of r_h for 12 Gyears for 3 values of ρ . The following values were used to create these curves:

$$\begin{aligned}\alpha &= .4, \\ \beta &= 10, \\ M_* &= 6000M_\odot, \\ m_a &= 30M_\odot, \\ r_{h,0} &= 1\text{pc}, \\ \sigma &= 5\text{km s}^{-1}.\end{aligned}$$

These correspond to the values used in Figure 1 in [3]. The agreement is not perfect, which may be due to the simple differencing scheme used here.

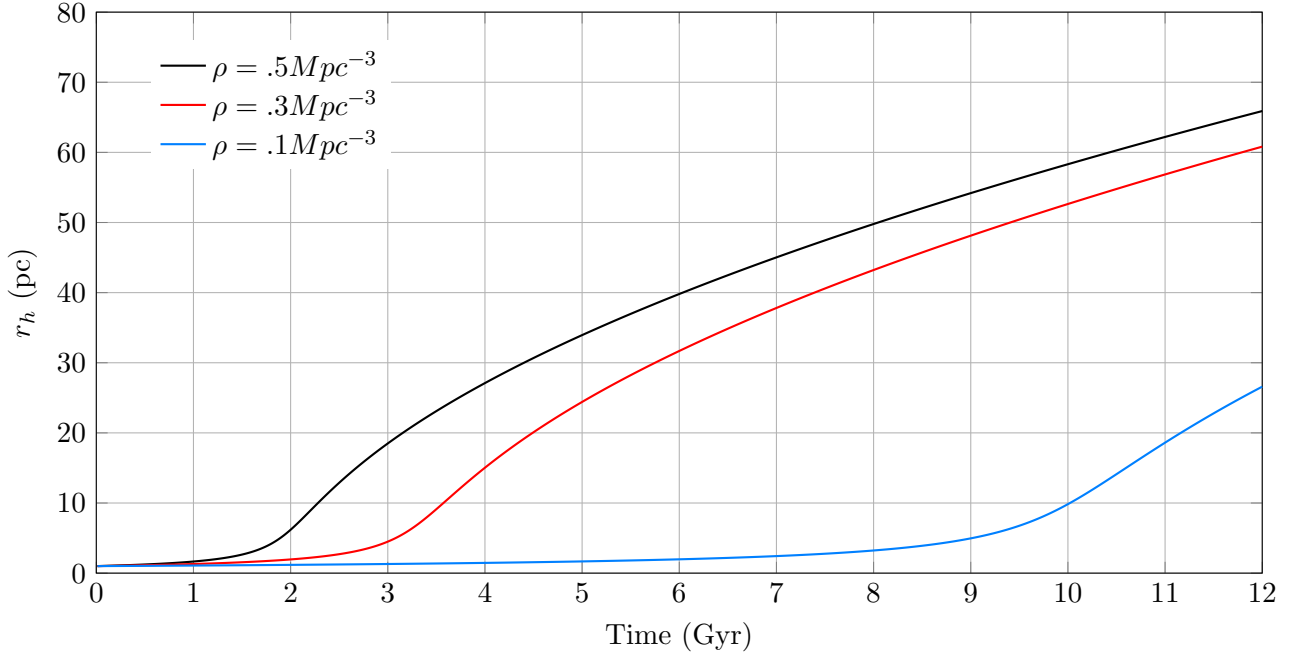


Figure 3: Dynamical heating of a 6000 M_\odot star cluster by 30 M_\odot MACHOs.

3 Conclusions

In the microlensing search, 17 microlensing systems are used and the results imply that Milky Way halo contains $\sim 20\%$ MACHOs. The optimized fraction is a factor of two smaller than found in the previous work in 1997[1], where only eight microlensing candidates were used, but the MACHO fraction is consistent within the error of the previous statistics. From this, we conclude that the fraction is in great tension with the microlensing samples. Also, the microlensing method depends on the halo density profile $\rho(r)$ and especially the dynamics of MACHOs, which may significantly influence the the duration of lensing effect t_i through

$$t_i = \frac{2u_{TH}R_E \cos \theta}{v_r} \quad (8)$$

where θ is the angle from the normal at which the MACHO enters the tube and v_r is radial velocity. In these works, the Maxwell-Boltzmann distribution is assumed for the velocity distribution. Alternatively, galaxy rotation curves may provide useful clues for the MACHO dynamic models. In addition, future multi-messenger observation may enables us to identify these MACHOs and make more realistic models and self-consistent constraints possible.

Figures 4 and 5 plot the solution of either half-light radii = 13 (starting from $r_H = 2$ pc), or $3\sqrt{2}$ (starting from $r_H = 13$ pc) of Eri II's globular cluster for cluster ages of 3 and 12 Gyr, respectively. Regions to the upper-right of the lines would be excluded because the cluster would have grown larger than its present size.

The dynamic heating constraints here are a function of measurables r_H (half-light radius, and distance), cluster visual composition and age (star luminosity, spectra). These parameters are likely to improve with planned instrumentation improvements (eg. the infrared James Webb telescope), which should enable continued increase number of appropriate structures and accuracy of the measurements. This will allow the restraints computed by this method to continue to be refined in the near- and medium-term future.

The measured parameters of the dynamic heating and gravitational lensing methods described here are fairly complementary so small differences in the increase of refinement rates should not immediately exclude one over the other.

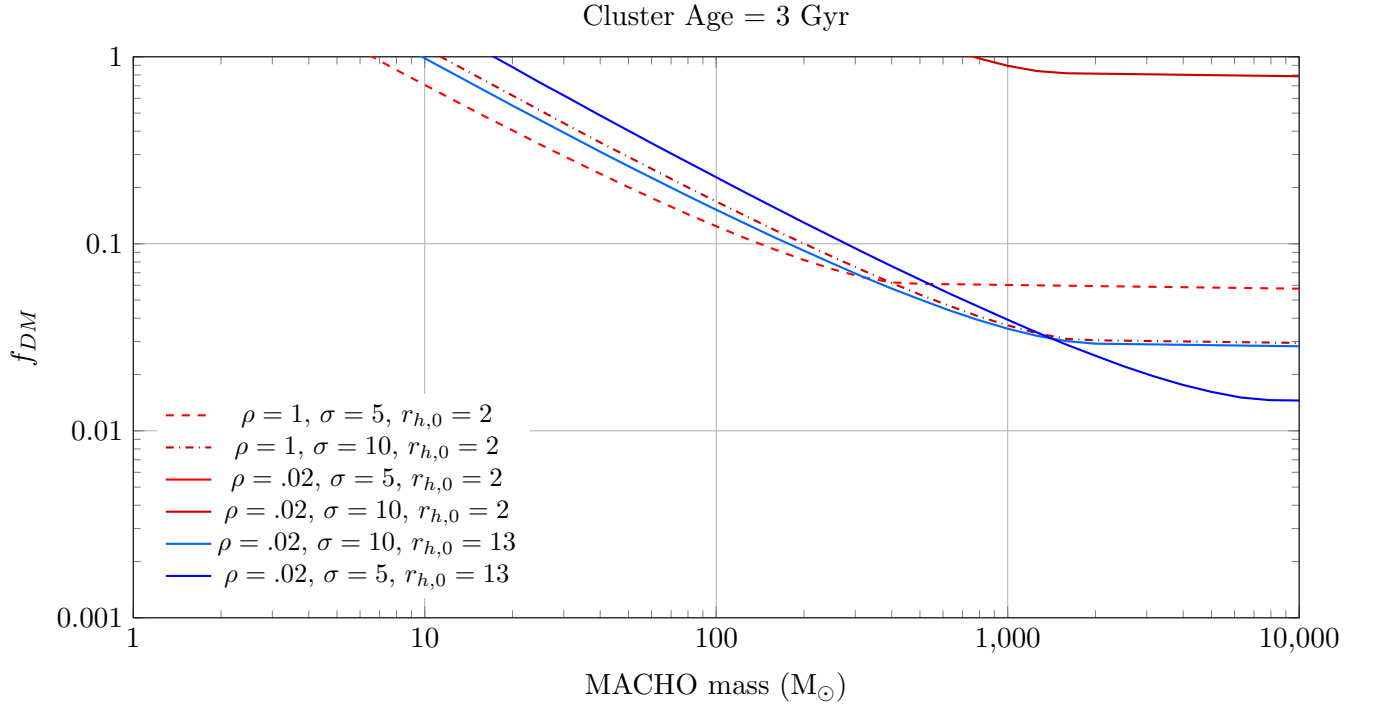


Figure 4: Excluded by cluster in Eri II (upper-right of lines)

References

- [1] Ch Alcock, RA Allsman, D Alves, TS Axelrod, AC Becker, DP Bennett, KH Cook, KC Freeman, K Griest, J Guern, et al. The macho project large magellanic cloud microlensing results from the first two years and the nature of the galactic dark halo. *The Astrophysical Journal*, 486(2):697, 1997.
- [2] Charles Alcock, RA Allsman, David R Alves, TS Axelrod, Andrew C Becker, DP Bennett, Kem H Cook, N Dalal, Andrew John Drake, KC Freeman, et al. The macho project: microlensing results from 5.7 years of large magellanic cloud observations. *The Astrophysical Journal*, 542(1):281, 2000.
- [3] Timothy D. Brandt. Constraints on macho dark matter from compact stellar systems in ultra-faint dwarf galaxies. *The Astrophysical Journal Letters*, 824(2):L31, 2016.
- [4] Kim Griest. Galactic microlensing as a method of detecting massive compact halo objects. *The Astrophysical Journal*, 366:412–421, 1991.

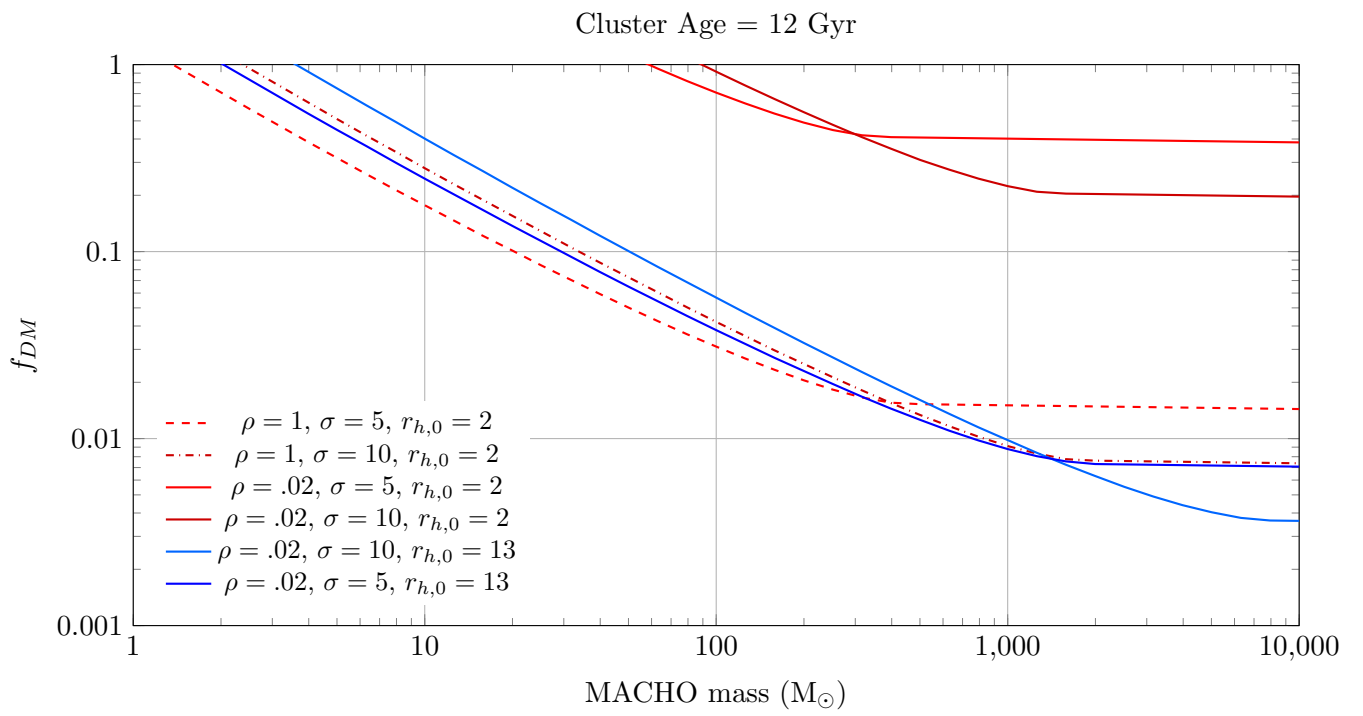


Figure 5: Excluded by cluster in Eri II (upper-right of lines)